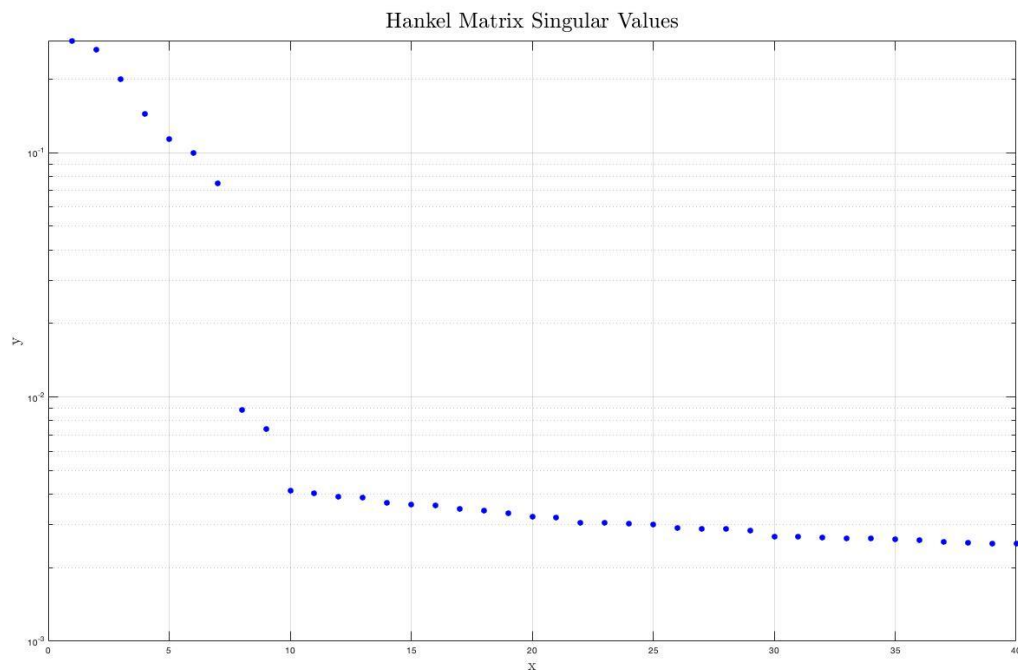


Peter Racioppo  
103953689

## Math 270A – Final Project

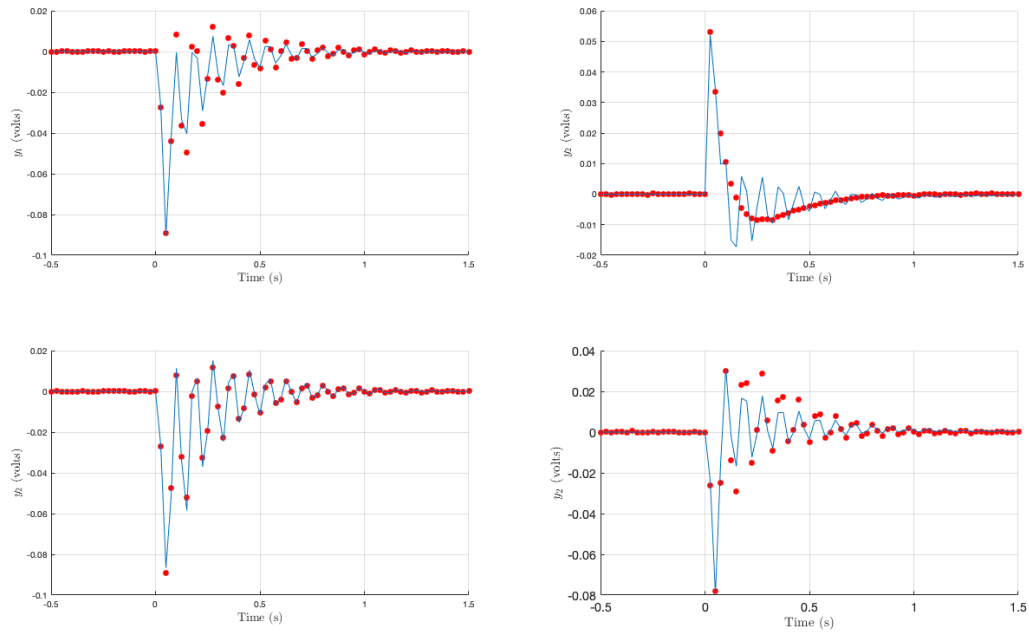
### Task #1: Model identification

(1) Hankel matrices were computed for models of dimensions  $\{6,7,10,20\}$ . The maximum modulus of the eigenvalues in each case were 0.9526, 0.9144, 0.9141, and 0.9977, respectively, indicating that each of the models is asymptotically stable. The singular values of the Hankel matrix for the 7-state model are displayed below, showing a sharp drop off in the magnitude of the first seven singular values and the remaining singular values.

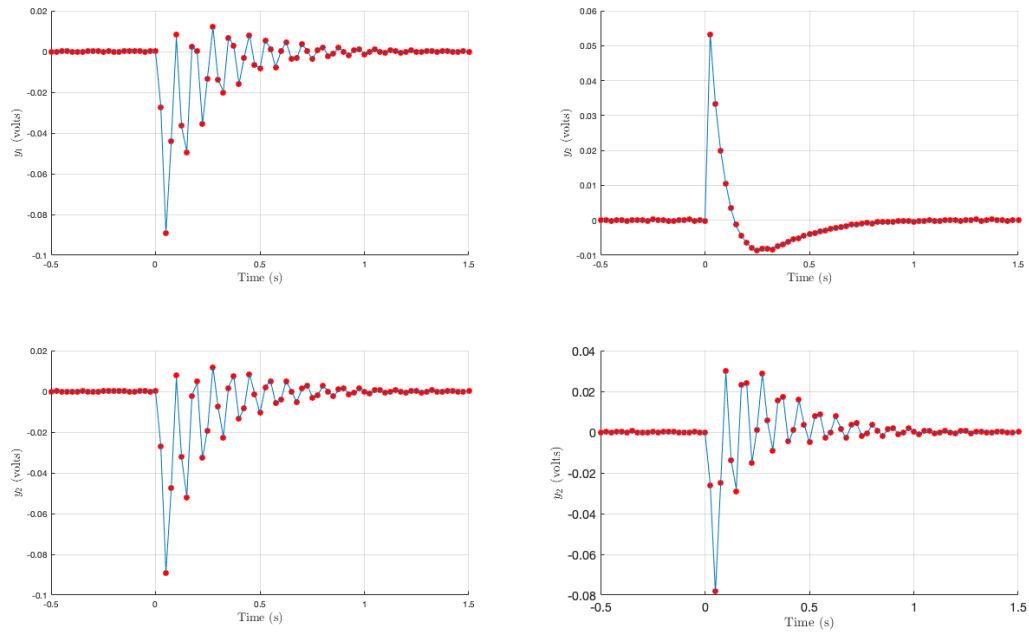


(2) The impulse response matrices were computed for each of the four models. The results are displayed below (11 component: top left, 12 component: top right, 21 component: bottom left, 22 component: bottom right).

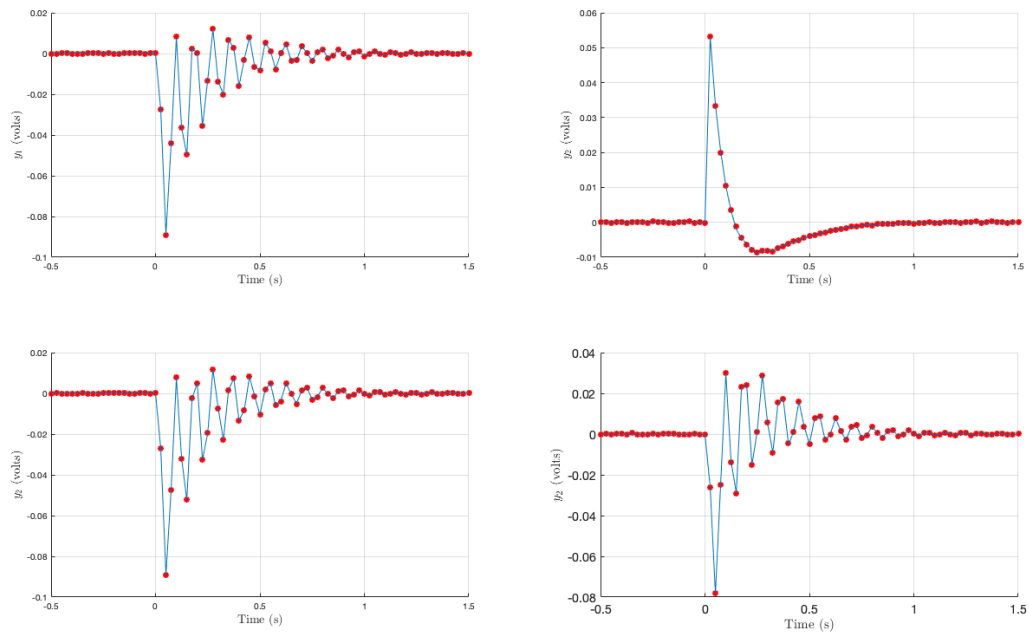
## Impulse Response – 6 State Model



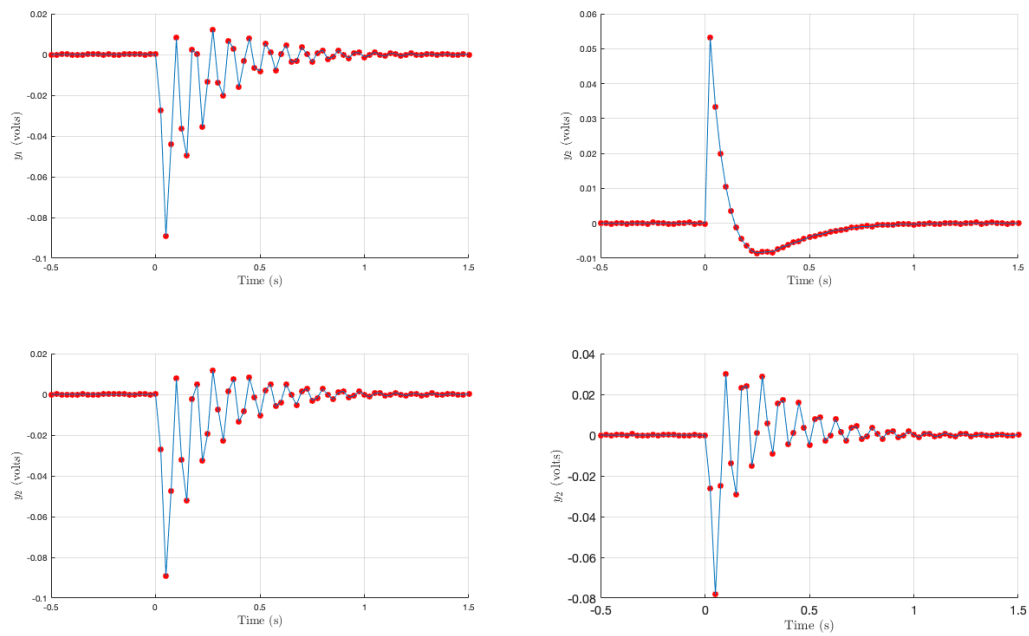
## Impulse Response – 7 State Model



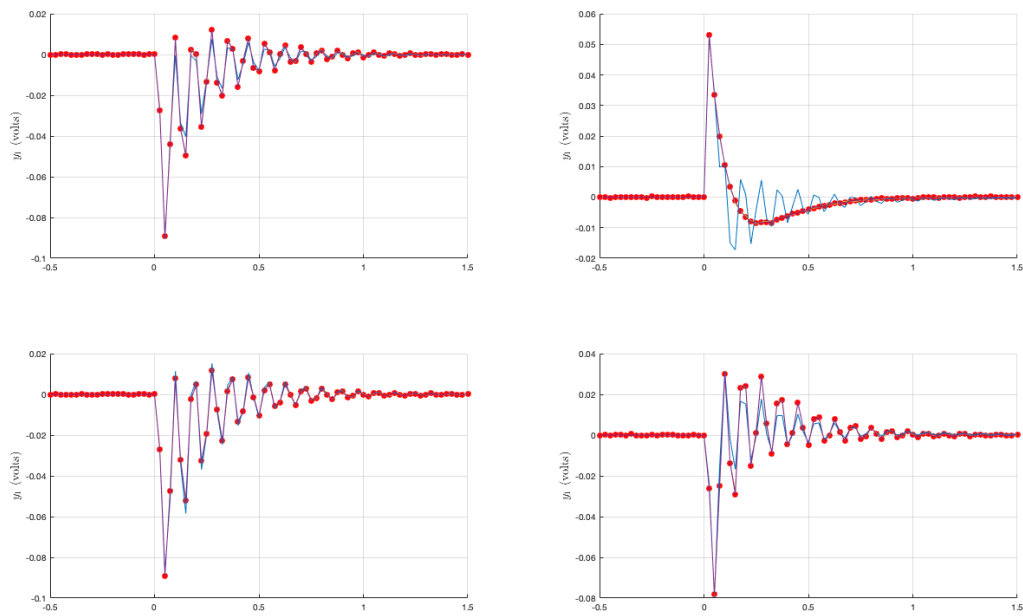
## Impulse Response – 10 State Model



## Impulse Response – 20 State Model



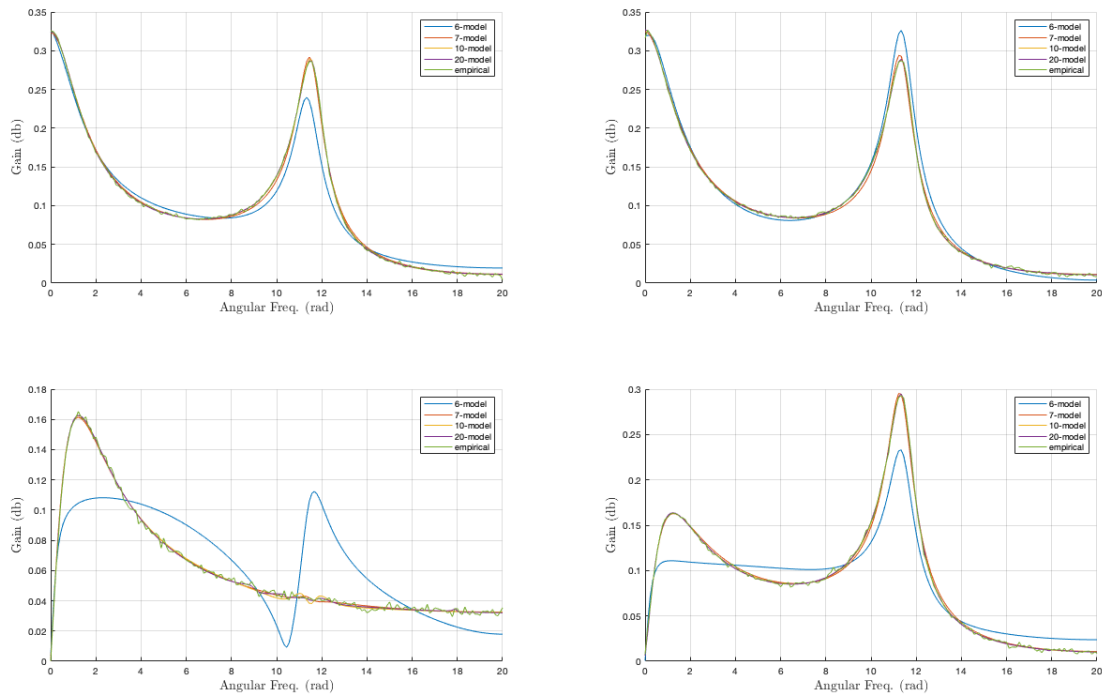
The impulse responses of all four models, plotted together for comparison



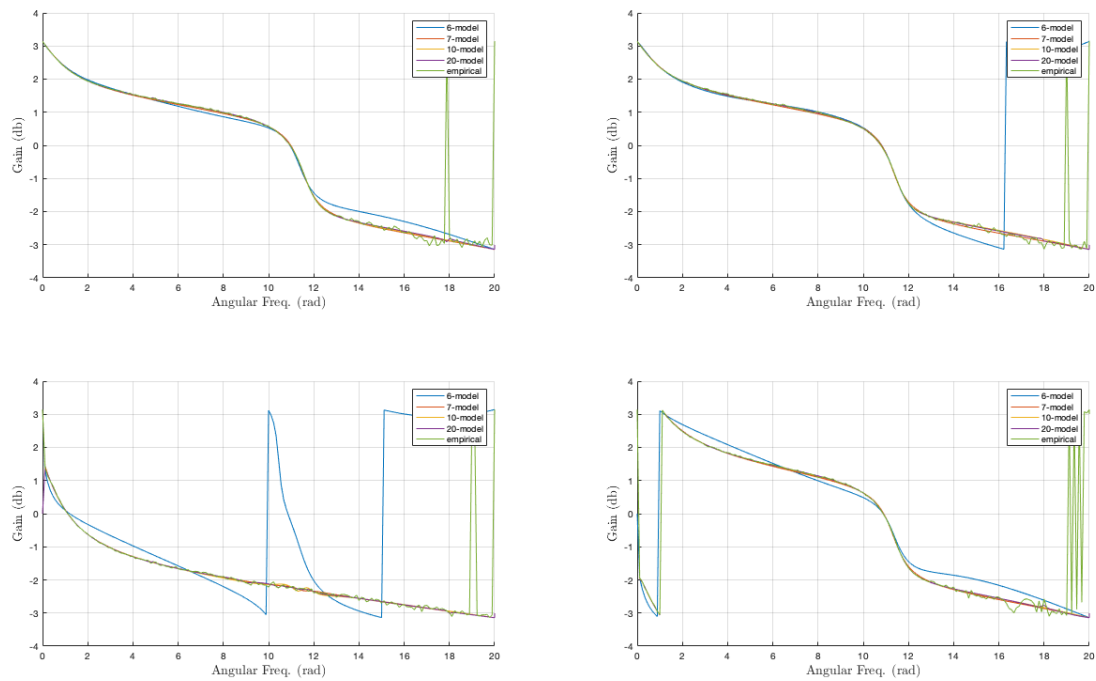
The 6-order model clearly has an inferior reproduction of the pulse-response data, while the others are essentially indistinguishable.

(3) – (4) The frequency responses matrices for each of the four systems were computed, and are plotted below along with the empirically estimated values (11 component: top left, 12 component: top right, 21 component: bottom left, 22 component: bottom right).

Magnitudes of the frequency responses for each channel, with empirical estimate



Phases of the frequency responses for each channel, with empirical estimate



(Units are db and rad/s)

As shown in the figures, all models of order 7 or higher, closely reproduce the empirical estimates, except for some spikes in the empirical estimates near the Nyquist frequency. The 6-state model does a significantly worse job of reproducing the results, particularly in the 21-channel.

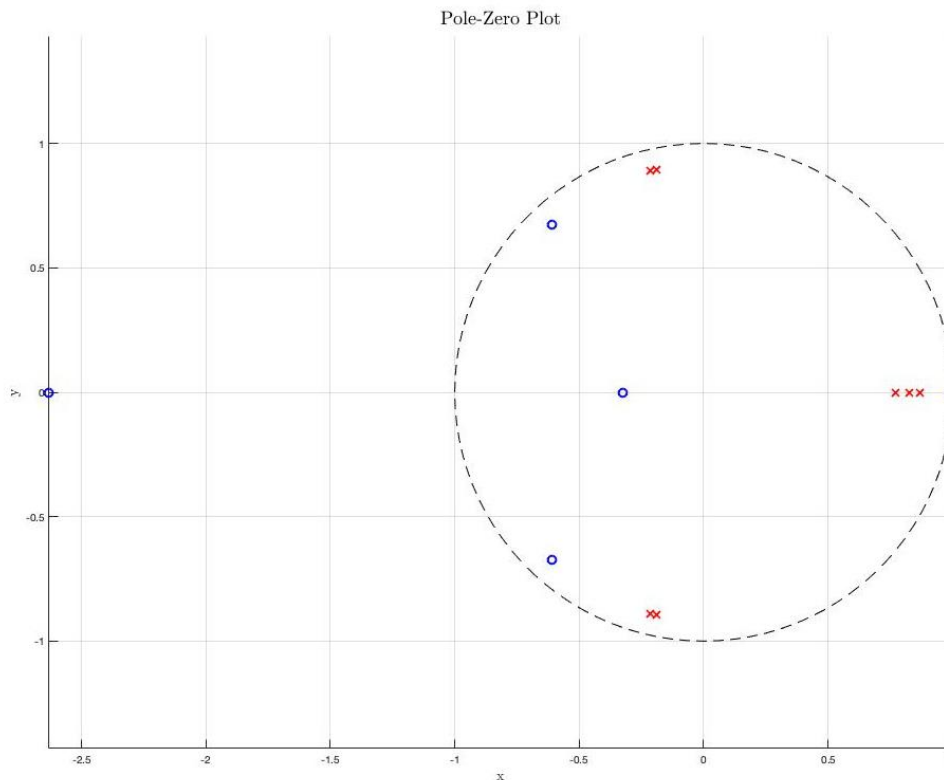
---

## Task #2: Transmission zeros of the MIMO model and zeros of each channel

(1) The five finite transmission-zeros of the 7-state model are (from largest to smallest mag.):  $-2.6310 + 0.0000i$ ,  $0.9988 + 0.0000i$ ,  $-0.6078 + 0.6740i$ ,  $-0.6078 - 0.6740i$ ,  $-0.3241 + 0.0000i$ .  $|z_1| > 1$ , but the other magnitudes are less than 1.

(2)

Graph of the poles and transmission zeros in the complex plane. Eigenvalues are denoted with an 'x' and transmission zeros with an 'o.'



(3)

The eigenvalues are:

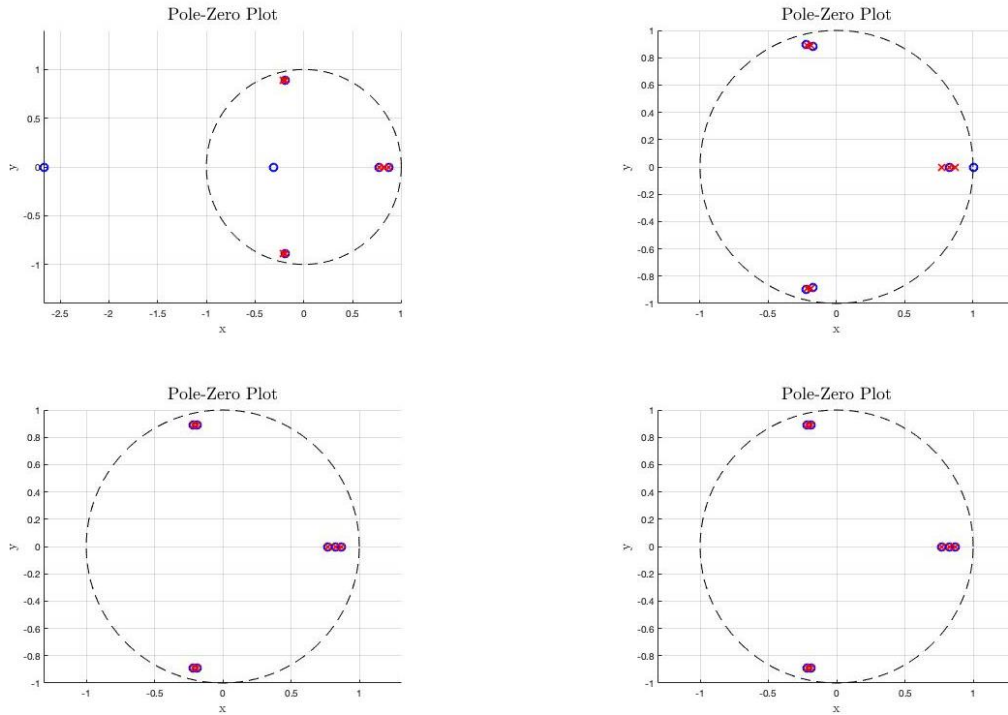
$-3.6842 + 71.1394i$ ,  $-3.6842 - 71.1394i$ ,  $-3.5800 + 72.2737i$ ,  $-3.5800 - 72.2737i$ ,  
 $-10.4604 + 0.0000i$ ,  $-7.6568 + 0.0000i$ ,  $-5.6364 + 0.0000i$

Three of the continuous-time eigenvalues lie on the real axis and the remaining four are two complex-conjugate pairs. There are 2 damped oscillators in the model. The natural frequency of

a pole corresponds to its modulus and the damping ratio to minus the cosine of its phase. The natural frequencies of the oscillators are 11.3374 rad/s and 11.5168 rad/s, which are near the peak gain of the 1,2 element of the frequency response.

(4)

Plot of the channel transmission-zeros



The Hankel singular values of each channel are:

HSV1 = [0.0415, 0.0264, 0.0156, 0.0000, 0.0000, 0.0000, 0.0000];

HSV2 = [0.0188, 0.0081, 0.0001, 0.0001, 0.0000, 0.0000, 0.0000];

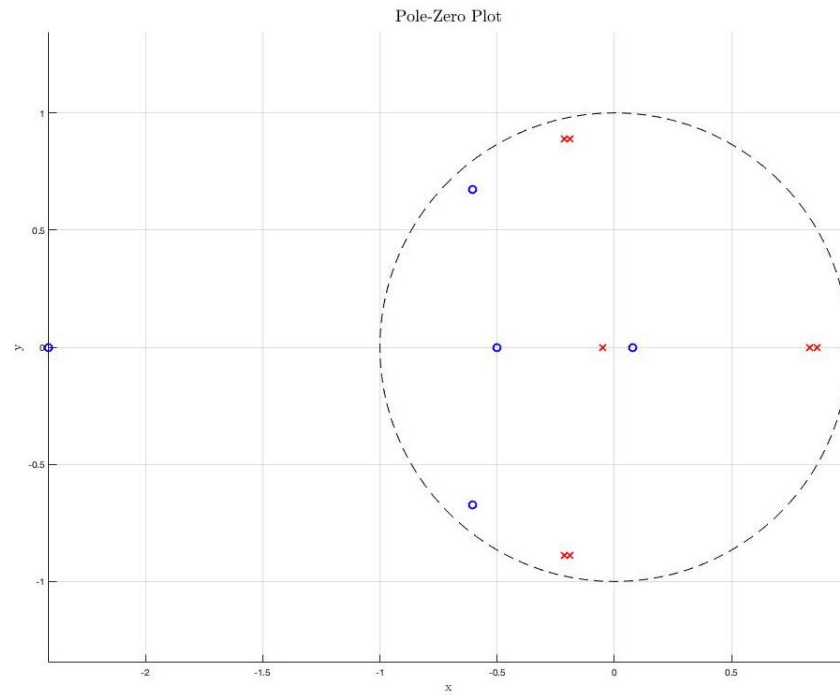
HSV3 = [0.0472, 0.0375, 0.0199, 0.0000, 0.0000, 0.0000, 0.0000];

HSV4 = [0.0382, 0.0376, 0.0128, 0.0063, 0.0000, 0.0000, 0.0000];

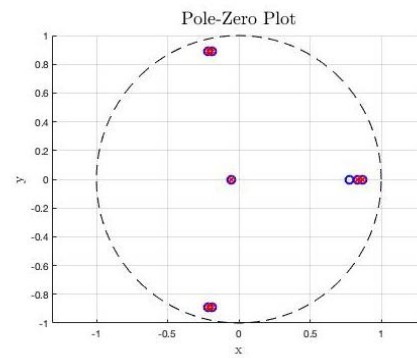
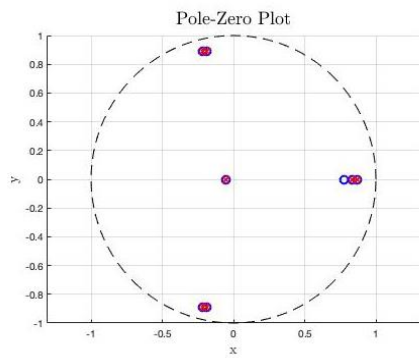
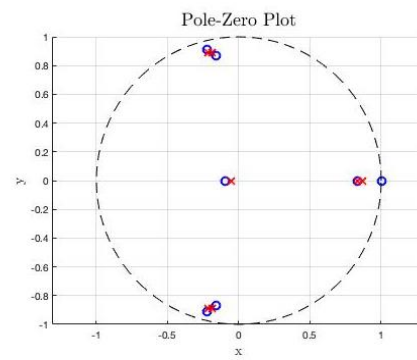
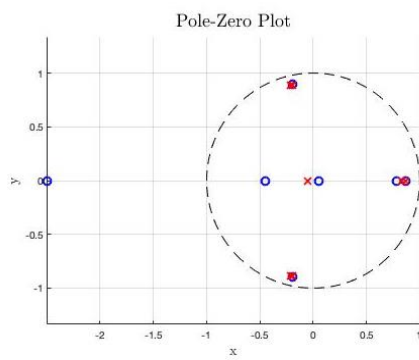
There are 4, 3, 4, and 3 zero-valued Hankel singular values in channels 1, 2, 3, and 4, respectively, corresponding, evidently, to the number of near pole-zero cancellations in each channel.

## (5) 8-state model

Plot of the eigenvalues and transmission zeros in the complex plane



Plot of the transmission-zeros for each channel



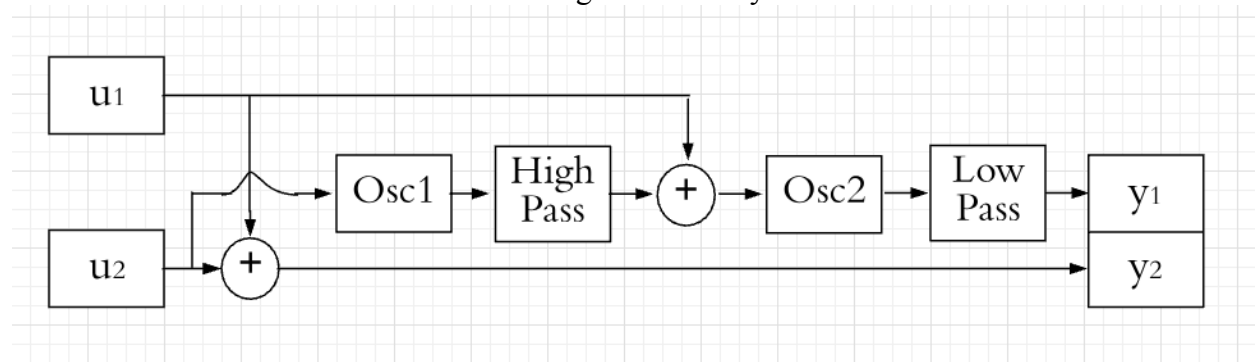


As can be seen from the plots, there is an additional zero in the pole-zero plot, near the origin, with an additional transmission zero in close proximity.

### Task #3: Block diagram from analysis of individual channels

There are 2 damped oscillators and 3 dampers in the system. In the 2,1 and 2,2 channels, all poles are canceled by transmission-zeros. The  $y_2$  output appears to be identical to either a  $u_1$  or  $u_2$  input. In the 1,1 channel, one of the pairs of complex-conjugate poles is canceled, while in the 1,2, neither is canceled. In the 1,1 channel, two of the poles on the real axis are canceled, while in the 1,2 channel, only one is canceled. The 1,2 channel has a zero with real part equal to 1. This zero can couple with one of real-valued poles to form a high-pass filter, while the other pole is a low-pass filter, and likewise there is a low-pass filter in the 1,1 channel. In summary, there is 1 oscillator and 1 low-pass filter in the 1,1 channel, while the 1,2 channel has these components along with another oscillator and a high pass filter. The block diagram for this setup is shown below. This analysis doesn't tell us the order of either of the two sets of oscillator and low/high pass filter. That is, Oscillator 1 could come before or after the high-pass filter, and Oscillator 2 could come before or after the low-pass filter. The existence of both a low-pass and a high-pass filter is evident in the plots of the magnitudes of the 1,1 and 1,2 channels in the frequency response. In these plots, the gains are high for very low frequencies, decrease with respect to frequency until about 8 rad/s and then increase and peak at about 11.3 rad/s.

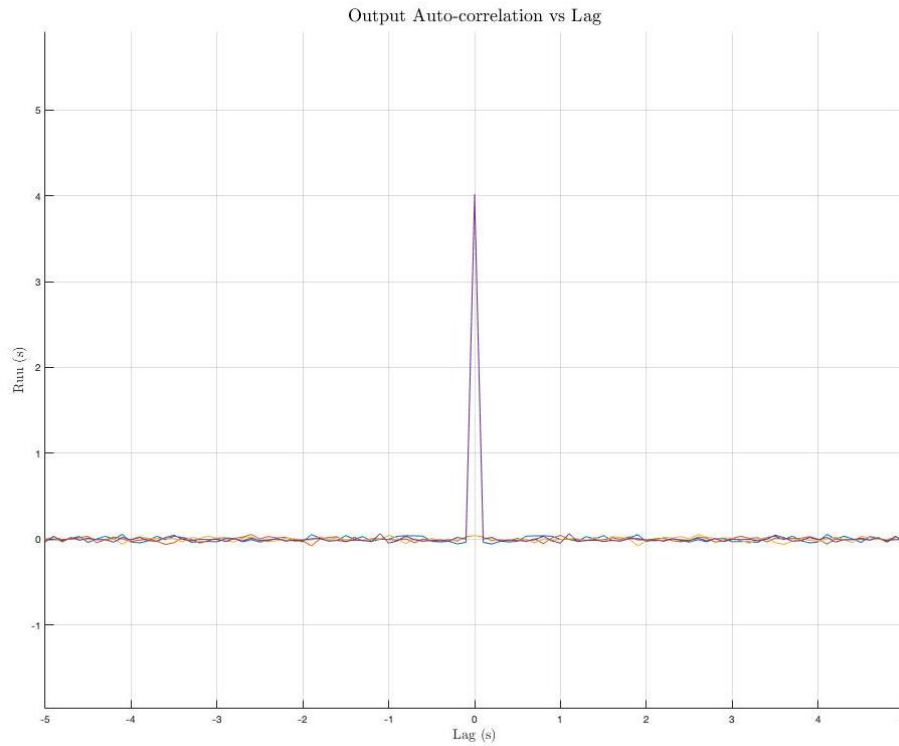
Block Diagram of the System



### Task #4: Impulse response identification from white noise inputs

(1) The input sequences have means  $-9.6619 \times 10^{-4}$  and  $0.0013$ , which are close to zero.

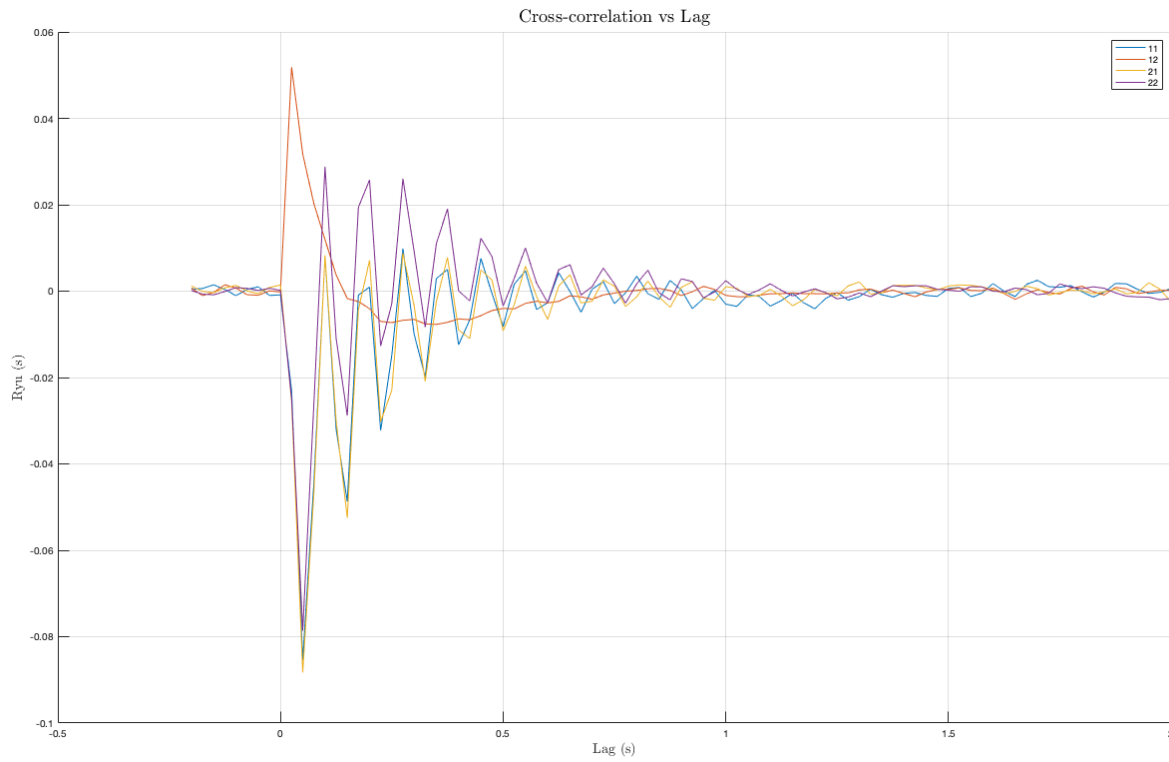
(2) Graph of the four elements of the autocorrelation  $R_{uu}$ , for lags between -5 and 5 seconds.



The autocorrelations are approximately zero everywhere except when the lag is approximately zero.

(3)  $R_{uu}[0] = [3.9855, 0.0437; 0.0437, 4.0194] \approx [4, 0; 0, 4]$

(4) Plot of the cross-correlation  $R_{yu}$  for lags between -0.2 and 2 seconds, with the {first, second} column of  $R_{yu}$  normalized by the variance of the {first, second} channel. The results are close to the experimental pulse responses.



### Task #5: $H_2$ norm analysis of identified model

(1)  $\|Y_{rms}\| = 0.2237$

(2)  $\|P\|_{H_2} = 0.0946$

(This value is different for some reason, though all 3 should be the same).

(3)  $\|Y_{rms}\|^2 = 0.0500$   
 $\|P\|_{H_2} = 0.2237$

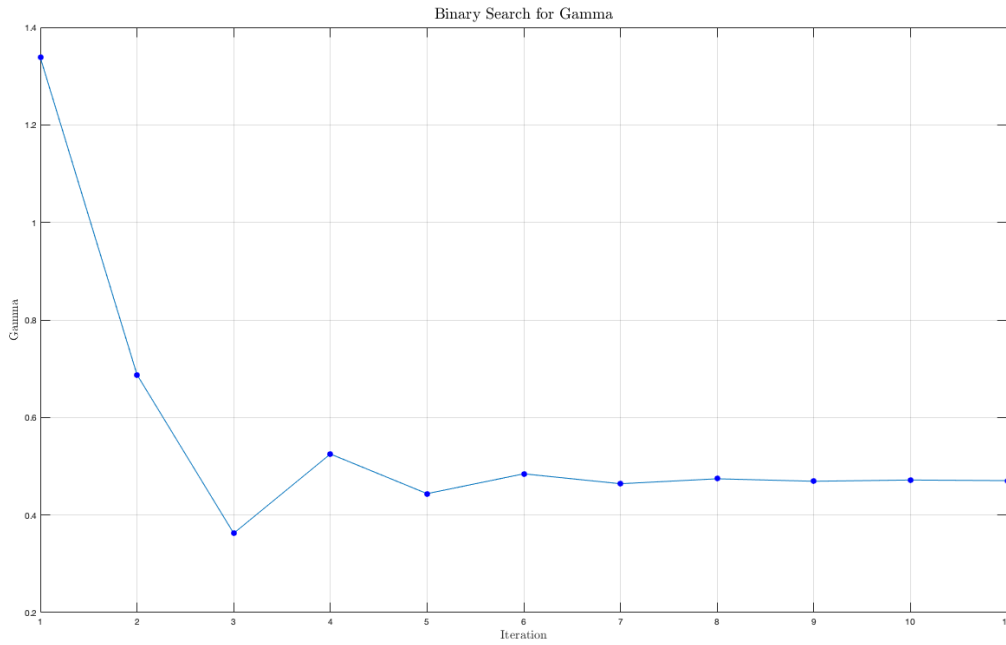
### Task #6: $H_\infty$ norm analysis of identified model

(1) – (3)

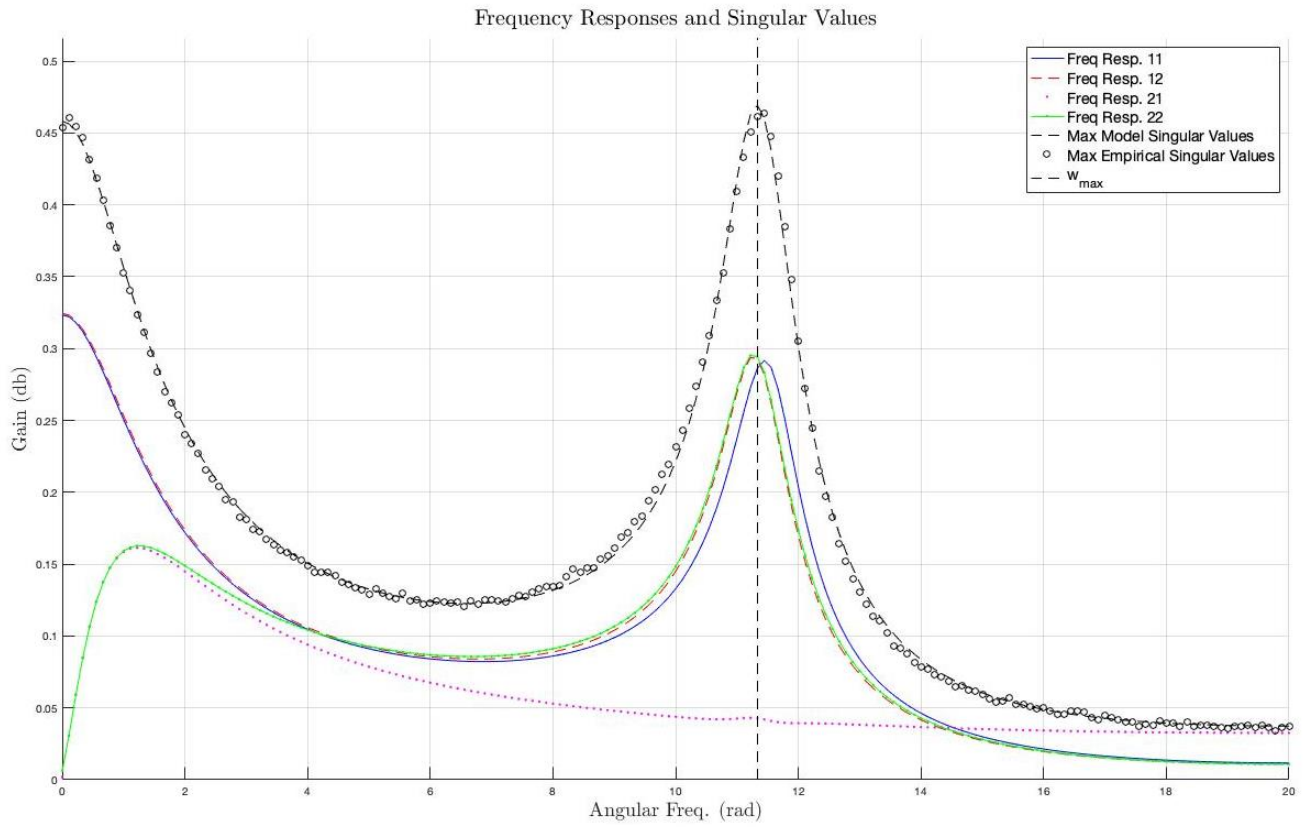
$\|P\|_{H_\infty} = 0.4705$

$\omega_{max} = 11.3356 \text{ rad/s}$

Plot of binary search procedure on gamma, used to find the H infinity norm of P



(4) Plot of the discrete-time frequency response of the identified model,  $w$  element of  $[0, w_{nyq}]$ .



The singular values of the model and empirical frequency responses, plotted with a dashed line, and circular markers respectively, closely match each other and bound all channels of the frequency response at all angular frequencies. The frequency  $\omega_{\max}$ , which maximizes the magnitude of the discrete-time frequency response is marked with a vertical line, and closely matches the peaks in the frequency responses.